On-chip micromanipulation and assembly of colloidal particles by electric fields

Orlin D. Velev* and Ketan H. Bhatt

Received 7th April 2006, Accepted 6th June 2006
First published as an Advance Article on the web 27th June 2006
DOI: 10.1039/b605052b

We overview the ways in which electric fields can be used for on-chip manipulation and assembly of colloidal particles. Particles suspended in water readily respond to alternating (AC) or direct current (DC) electric fields. Charged particles in DC fields are moved towards oppositely charged electrodes by electrophoresis. Dielectrophoresis, particle mobility in AC fields, allows precise manipulation of particles through a range of parameters including field strength and frequency and electrode geometry. Simultaneously, DC or AC electrokinetics may drive liquid flows inside the experimental cells, which also leads to transport and redistribution of the suspended particles. Examples of dielectrophoretic manipulation and assembly of nanoparticles and microparticles by planar on-chip electrodes are presented. The structures assembled include conductive microwires from metallic nanoparticles and switchable two-dimensional crystals from polymer microspheres. We also discuss how dielectrophoresis and AC electrokinetics can be used in droplet-based microfluidic chips, biosensors, and devices for collection of particles from diluted suspensions.

The area of electrokinetics has seen rapid growth recently in part because of the increased interest in processes and devices that allow manipulation and assembly of structures from micro- and nanosized particles. Advances in microfabrication, microfluidics and the thrust in multidisciplinary research have spanned off studies of small electrically controlled devices targeted for applications such as manipulation of live cells and biomacromolecules, characterization of minuscule liquid samples, massively parallel bioassays and assembly of nanostructures with electronic or photonic functionality. This review discusses how colloidal particles suspended in water can be manipulated with ''on chip'' electrodes energized by alternating (AC) and constant (DC) electric fields.

Department of Chemical & Biomolecular Engineering, North Carolina State University, Raleigh, NC, 27695, USA. E-mail: odvelev@ncsu.edu; Fax: +1 919 515-3465

The first advantage of using electric fields to manipulate and assemble particles on a chip stems from the ability to precisely tune the forces exerted on the particles by the field and the field-induced particle–particle interactions. The parameters characterizing an AC signal applied to electrodes include magnitude, frequency, wave shape, wave symmetry, and phase (when multiple electrodes are involved). All of these parameters can be controlled electronically and all can influence in different ways the behaviour of particles between the electrodes. This allows precise adjustment of the driving forces to an extent that is hardly possible with any alternative technique using liquid flow, evaporation, sedimentation or mechanical manipulation. The second major advantage of using electric fields on a chip is the relative simplicity and availability of the experimental cells and equipment needed. The microlithography facilities used in electronic circuit fabrication allow facile fabrication of any kind of ''chips'' with microelectrodes for

Orlin Velev

Orlin Velev leads a research group at NCSU which studies and develops nanostructures with electrical and photonic functionality, biosensors and microfluidic devices. He has been one the first to synthesize ''inverse opals'', colloidosomes, develop microscopic biosensors and discover novel types of self-assembling microwires. He has contributed more than 75 publications, which have been cited more than 2500 times. For more information see http://crystal.che.ncsu.edu/

Ketan Bhatt

Ketan Bhatt received his BE (Honors) degree in chemical engineering from Birla Institute of Technology and Science, Pilani, India in 2001. He received his PhD in chemical engineering from North Carolina State University in 2006. His graduate research was devoted to the on-chip manipulation and controlled assembly of colloidal particles using alternating electric fields.

this type of research.[1] The interfacing of the chips to the control circuitry is done by direct electrical contact and there are no mechanical or optical components involved (except for observation purposes). In contrast, for example, manipulation of particles by optical means requires the construction of laser traps that include complex mechanical, optical and electronic components.

Harvesting the convenience of electrical particle manipulation, however, requires knowledge and prediction of the response of the particles and liquid inside the experimental cells to the fields applied to the electrodes. That response is often quite complex, as generally, electric fields drive motion of both particles and liquid as will be explained in more detail below. Rich varieties of field-driven effects have been revealed and are the subject of active investigation. We exemplify these processes for the simplest experimental "chip" consisting of two parallel electrodes deposited on a surface. An overview of the processes taking place under the action of DC and AC fields in this system is presented in Fig. 1. The mobility of the particles can be a result of forces acting directly on them or of the drag from the moving liquid around them. The electric field driven mobility of the particles and of the liquid can be classified in four broad categories (Fig. 1a–d).

The electrophoretic mobility of charged particles in constant electrical fields has been, for a long time, a major topic in colloidal science.[2] Charged particles in water are surrounded by a cloud of counterions, and the particle–counterion complex is electroneutral. The ions in the fluid layer closest to the interface are strongly attracted to the substrate and are hence immobile. This layer is known as the Stern layer. The application of external field, however, can "shear" away some of the ions outside this layer, which begin moving towards the electrode of opposite charge. The particle surface below the plane of shear is characterized with a potential in that plane called zeta potential, ζ. This potential is involved in nearly all electrokinetic flows.[3] The particles of effective potential ζ move towards the electrode of opposite sign (Fig. 1a). The major electrophoretic characteristic of the particles is the electrophoretic mobility, μ, defined as the coefficient of proportionality between the electric field intensity E and particle velocity u.

$$\mu = \frac{u}{E} \tag{1}$$

The electrophoretic mobility increases with the particle zeta-potential and decreases with the viscosity of the media, η. The exact coefficient of correlation between μ and ζ depends on the size of the particles. The mobility of a "small" particle defined as having radius r much smaller than the Debye length of the counterionic atmosphere, $1/\kappa$, is described by the Hückel equation

$$\mu = \frac{2\,\varepsilon\,\varepsilon_0\zeta}{3\,\eta} \tag{2}$$

where ε and ε_0, are the dielectric permittivity of the media and vacuum, respectively. The electrophoretic mobility of particles of size much larger than the Debye length of the counterionic layer ($r \gg 1/\kappa$) is given by the Helmholtz–Smoluchowski equation

$$\mu = \frac{\varepsilon\,\varepsilon_0\,\zeta}{\eta} \tag{3}$$

Tabulated values for the numerical coefficient in the right hand side of these equations for the case of particles of size comparable to the Debye length are available in the literature.[4] The electrophoretic mobility of non-spherical particles is dependent on their orientation in the applied field. For cylindrical particles oriented in the direction of the electric field, the electrophoretic mobility is given by eqn 3, whereas for particles oriented perpendicular to the electric field the numerical coefficient has been obtained by Ohshima.[5]

The electrophoretic mobility determined by measuring the particle velocity as a function of the applied external field allows measuring the particle ζ-potential. O'Brien and White broke down the problem of calculating zeta potential from the electrophoretic particle mobility into two simpler problems,[6] *viz.* calculation of force required to move a particle with velocity u with no applied field and the force required to hold the particle fixed in the presence of an electric field E. These analytical tools helped them to develop a numerical scheme for the conversion of particle mobility measurements into zeta potential values for spherical particles. The actual velocity of a charged particle in a real experimental situation of two electrodes inside a cell, however, is going to be equal to the theoretical one only in a very limited volume, where the liquid in the cell is immobile.

A common complication in using DC fields to move particles in ionic media (such as water) is the electrophoretic mobility of the liquid adjacent to the walls of the experimental cell. The dielectric walls of chips and containers in contact with water nearly always develop a surface charge, with the corresponding counterionic double layer in the water phase. The ions in this layer move towards the oppositely charged electrode, dragging the liquid, and resulting in electroosmotic water motion (Fig. 1b). The electroosmotic velocity of the liquid adjacent to the wall is well approximated by the Helmholtz–Smoluchowski eqn (3), albeit with a negative sign. The electroosmotic effect is conveniently utilized in

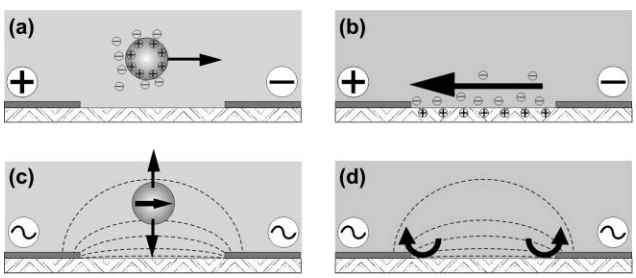

Fig. 1 Schematics of the four groups of electric field driven effects that can be used for on-chip manipulation of particles in suspension. (a) Electrophoresis—particles migrate towards the electrode of opposite charge in DC field. (b) DC electroosmosis—liquid flows are driven by the moving counterionic layer near the wall between the electrodes (dragging the particles along). (c) Dielectrophoresis—the particles are attracted or repelled by the areas of higher AC field intensity. (d) AC electro-hydrodynamics—liquid flows are generated at the walls near the electrodes by the gradient of the field.

microfluidic pumps,[7] but could also be a nuisance in the case of particle manipulation. The velocity of the particles will be equal to the one caused by the electrophoretic effect, plus the electroosmotic velocity of the surrounding liquid (which changes with the position inside the cell). Thus, the moving liquid can drag the particles in arbitrary direction or distort assembled structures. The assembly process can also be disrupted by electrolysis. For this reason, DC electrophoresis is seldom used as a means of transport of particles. Faradaic reactions on electrode surfaces at low frequency AC fields may as well lead to diverse electrokinetic effects when particles are present[8] (discussed in more detail below).

The practical alternative is to manipulate the particles using alternating fields. The application of an AC field across particle suspensions leads to emergence of dielectrophoretic (DEP) force. As the sign of the electrode polarization changes constantly, the particles are not attracted by direct charge–electrode electrostatic interactions (apart from oscillations at low frequencies on the order of tens of Hertz). Instead, the DEP force arises *via* interaction of the induced dipoles with the gradient of the (inhomogeneous) field. The resultant force, F_{DEP}, is dependent on the gradient of the field squared, ∇E^2 and the particle radius cubed (*i.e.*, proportional to particle volume),[9–13]

$$F_{DEP} = 2\pi\varepsilon_1 \mathrm{Re}|\underline{K}(\omega)|r^3\nabla E^2 \quad (4)$$

Its sign and magnitude are dependent on the effective polarizability of the particle, which is described by the real part of the Clausius–Mossotti function, *K*,

$$\mathrm{Re}|\underline{K}| = \frac{\varepsilon_2-\varepsilon_1}{\varepsilon_2+2\varepsilon_1} + \frac{3(\varepsilon_1\sigma_2-\varepsilon_2\sigma_1)}{\tau_{MW}(\sigma_2+2\sigma_1)^2(1+\omega^2\tau_{MW}^2)} \quad (5)$$

In the above formulae, ε_1 and σ_1 are the dielectric permittivity and conductivity of the media and ε_2 and σ_2—that of the particles. Metallic and other highly polarizable particles are always attracted along the gradient to the regions of high field intensity. It is important to note, that the major contribution to the low frequency polarizability of almost any type of particle dispersed in water comes from the conductance of the counterionic layer near the surface. Even though dielectric particles have lower bulk polarizability, they almost always have charge in water, so at low frequencies $\mathrm{Re}(K) > 0$ and the particles are attracted to the high field intensity areas. *K* changes sign (*i.e.*, the DEP force changes from attractive to repulsive) at a crossover frequency of $\omega_c = \tau_{MW}^{-1}$, where τ_{MW} is the Maxwell–Wagner charge relaxation time, $\tau_{MW} = \frac{\varepsilon_2+2\varepsilon_1}{\sigma_2+2\sigma_1}$. This frequency-dependent change of sign of the force is commonly observed with polymer microspheres in water[9–12] and allows a high degree of control *via* the field frequency. Zhou *et al.* have developed a numerical model to calculate the strength of the field-induced dipole in particles using the electrokinetic theory of Mangelsdorf and White[14,15] and obtained $\mathrm{Re}(K)$ values for both static and oscillating fields.[16] Furthermore, the dynamic double layer impedance is frequency-dependent, which can alter the strength and the shape of the electric field distribution near the electrodes, shifting the locations of the field maxima and minima as functions of the frequency.[17]

The dielectrophoretic force is not limited to AC fields. The largest possible magnitude of the induced dipoles will be realized in DC fields and DEP effects will be present in inhomogeneous fields in electrophoretic cells. The use of DC dielectrophoresis, however, is impractical, due to the much smaller magnitudes of the fields that could be applied in aqueous media. The use of AC voltage, on the other hand, allows manipulation of virtually any type of particle in any type of media and has the advantage of permitting high field strengths without water electrolysis and strong electroosmotic flows. Additional degrees of transport and manipulation can be offered by the use of travelling waves and rotating fields created by applying phase-correlated signals to arrays of electrodes. One of the best-known and widely used related effects is electrorotation, where the particles spin because of the interaction of the induced dipole and a rotating field created by multiple electrode pairs.[10] Electrorotation has been used, for example, in the characterization of the dielectric properties of live cells as a function of their viability and environment.[18–21]

The DEP effects become much more complex (and interesting) when large numbers of particles are present between the electrodes. The processes of interaction and assembly of the particles can be explained in an intuitively clear, albeit simplified, way by assuming that the field induces a dipole within each particle. These induced dipoles interact not only with the external field, but also with each other if the particles are close enough. The biggest energy gain is realized when the particles align in chains along the direction of the field lines. This "chaining" force, F_{chain}, is dependent on the field strength, *E*. A generalized expression for the force between adjacent particles is

$$F_{chain} = -C\pi\varepsilon_1 r^2 K^2 E^2 \quad (6)$$

where the coefficient *C* ranges from 3 to $>10^3$ depending on the distance between the particles and the length of the particle chain.[10] Particles of the same type always align along the field lines, regardless of whether their polarizability is higher or lower than the media, while mixtures of particles of lower and higher polarizabilities than the media could form alternating chains in the perpendicular direction.[22] Dipolar chaining and 3D structuring have been first observed and studied in relation to electrorheological fluids, and are presently a major tool in the assembly of organized particle materials and various structures and devices. A similar principle is used in electro-coalescence and large scale industrial separation of water droplets from crude oil.

The polarized particles not only interact with each other but also modify the field intensity in the region of the experimental cell. Our research in different types of dielectric and metallic particles has shown that the phenomena observed in suspensions of colloids could be further categorized in two basic classes. Illustration of these two distinctive cases of dielectric and conductive particles is presented in Fig. 2. The colour-coded plot of the simulated intensity of the field allows easy visualization of the direction and range of the forces that arise within the system. Dielectric particles with effective permittivity higher than the medium will be attracted in the

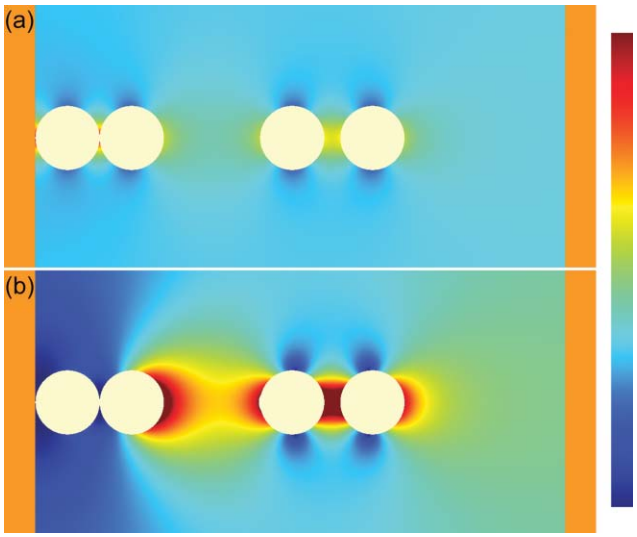

Fig. 2 Simulation illustrating the two general cases of electric field intensity distribution in chambers with colloidal particles. (a) Dielectric particles (ε = 5) and (b) conductive particles, suspended in a medium with lower relative dielectric permittivity ε = 2. The orange bars on either side represent the electrodes. The simulation demonstrates how the particles attract each other in chains, due to the high field intensity area in-between them (analogous to chaining force). However, conductive particles near electrodes also modify the electric field distribution in the whole chamber by extending the electrode into the solution (left pair in b); consequently the pattern of assembly of conductive particles is different.

direction of the higher intensity (warmer colours in Fig. 2a). The simulation shows how the field intensity between two polarizable particles increases and the particles move towards each other (similarly to the predictions based on dipole–dipole interactions, eqn 6). The disturbances of the field around the particles, however, are relatively minor, regardless of the position of the chain within the chamber.

The application of an electric field across a suspension of conductive (typically metallic) particles creates a different electrostatic pattern in the cell. The metallic particles are nearly infinitely polarizable, and the Clausius–Mossotti factor takes its limiting value of K = 1. The DEP and chaining forces are maximized. In addition, particles at the electrode edges will connect to the electrode, effectively extending it to the outer end of the particle chain (see the simulated example in Fig. 2b). The tip of the conductive chain formed will distort the field intensity across the whole cell, and establish a gradient towards the end particle. Other particles will then be attracted to the tip, extending it further out into the suspension in the direction of the other electrode. The conductive chain of metallic particles will keep on extending until the electrodes become short-circuited. A similar process of dielectrophoretic growth of metal nanoparticle wires that we reported earlier is described in detail further down in this paper. Another example of such a process is demonstrated by a study where gold nanoparticles form a pearl chain between electrodes separated by micron sized gaps.[23]

Uniform AC fields applied normally or tangentially to a charged wall do not engender fluid flows as the DC fields. Fluid flows, however, are generated in areas near the electrodes where a strong electric field gradient exists across a solid–liquid interface. The interaction of the ions collected in the high field intensity areas and the field leads to liquid drag near the dielectric wall adjacent to the electrodes. These flows, referred to as AC electrokinetic, are strongly dependent on the field frequency and electrolyte concentration because of their dependence on the capacitive charging of the double layer. The counterions farther away from the interface than the shear plane are loosely bound and have the ability to move in both the transverse as well as parallel directions. The external applied voltage at electrode surfaces modifies the native charge on the surface thereby leading to an "induced" zeta potential different from the intrinsic zeta potential. Furthermore, for AC fields the induced double layer charge changes sign synchronously with the electric field frequency. The counterions in the double layer move in and out of the layer during the subsequent half-cycles of the electric field frequency. This leads to induced zeta potentials that may be different for the positive and negative half-cycles of the AC field, but are always of sign same as that of the electrode field applied to the electrodes.[1] There is no net flow, unless the field has a component tangential to the surface. The ions in the double layer then react to tangential electric fields leading to bulk liquid flow along the interface. Notably even though an AC field is applied, the bulk flow in different half cycles points in the same direction along the field gradient resulting in a net fluid flow. This phenomenon is referred to as AC electro-osmosis or AC electrohydrodynamic (EHD) flow. As the applied electric field induces double layer formation and then leads to bulk fluid flow by acting on its own induced charge, these flows are also referred to as "induced-charge electro-osmosis (ICEO)".[24,25] AC EHD and electroosmosis are types of ICEO flows. The AC EHD flow velocity is given by

$$u = -\frac{\varepsilon \varepsilon_0 \zeta_{\text{ind}}}{\eta} E_{\text{t}} \tag{7}$$

where, ζ_{ind} is the induced zeta potential due to the applied external field and E_{t} is the tangential component of the electric field.[26,27] The AC electrokinetic flows can be used in microfluidic pumping and in techniques for on-chip manipulation and collection of particles.

Various techniques for particle manipulation and assembly have been based on combinations of the forces and effects overviewed above. Processes and applications reported by various researchers and by our group are reviewed in more detail in the following sections.

Electrophoretic particle manipulation and assembly

The ability to drive the particles towards an oppositely charged electrode can be used for their concentration, deposition or colloidal crystallization. If the field is strong enough, the particles can also be attached irreversibly to the surface. One of the first processes for electrophoretic deposition of ordered arrays of gold and latex particles onto surfaces of conductive carbon-coated copper grids under the action of electric field of 1–5 V cm^{-1} has been reported by Giersig and Mulvaney.[28] Adsorption, nucleation and growth of polycrystalline arrays have been observed with increasing periods of time. Multilayer

latex arrays have formed at higher field strengths. Such processes can be used to crystallize the particles by concentrating them near electrodes. The technique can be viewed as speeding up the deposition of dense particle crystals that would otherwise be formed under gravity. Wide cells are usually used in order to decrease the magnitude of electro-osmotic flows.

Direct electrophoretic control of the deposition speed of silica spheres for the fabrication of high quality crystals has been reported by Holgado *et al.*[29] DC field applied in the vertical direction in cylinders with sedimenting spheres, has been used to control the speed at which the spheres deposit on the bottom. The vertical electrophoretic mobility of the spheres can add up to the Stokes sedimentation velocity so crystals from small spheres can be assembled rapidly. When the field is applied in the opposite direction, it can slow the downward mobility of large spheres whose Stokes sedimentation speed is too high in order to slowly grow well-ordered crystals. Electrophoretic deposition of colloidal particles has been used to prepare various crystals and multilayered deposits.[30–39] Electrophoretic redistribution of encapsulated particles has been used in ''electronic ink'' and flexible displays.[40,41]

The dynamics of the electrophoretic assembly of latex particles suspended between conductive electrodes have been reported by Trau *et al.*[42,43] and Böhmer.[44] The latex particles are attracted to the oppositely charged electrode and the counterionic atmosphere around the particles disturbs the concentration polarization layer at the electrode surfaces. This leads to electrohydrodynamic flows around the particles that in effect pull them together to form 2D colloidal crystals at the electrode surface.[8,43,45–48] Alternatively, if the latex particles are confined into a thin gap of the order of their diameter, then AC fields can be used to organize 2D crystals by induced dipolar repulsion.[49–58] Richetti *et al.*[49] were the first to assemble ordered 2D aggregates from latex spheres confined in thin cells using alternating electric fields. Similar research has been carried out by the groups of Saville[54,55] and Marr.[56–58] In a more complex application, the photosensitivity of indium–tin oxide semiconductor layers has been used to optically pattern colloidal crystals.[59]

The electrohydrodynamic flows generated around the particles are a function of the electrolyte concentration and the frequency of applied field. Depending on these parameters, the electrohydrodynamic flows in the vicinity of the particles can aggregate them or separate them. Sides and co-workers have treated these phenomena theoretically and demonstrated experimentally how the critical frequency for the change in electrohydrodynamic flow direction depends on the particle size.[60–65]

Dielectrophoretic manipulation and assembly of nonconductive particles

This research area is by far the largest and best developed, due to the convenience and precision of the dielectrophoretic techniques. The potential of devices with various electrode configurations to move, rotate and separate dielectric particles has been recognized for more than 50 years. Many of the pioneering works and much of the research today are focused on the manipulation of DNA[66–72] and live cells.[73–85] The frequency-dependent cell membrane polarizability depends on a variety of factors and can be used to separate streams of live and dead cells and cells of different genotype in flow-through devices.[74,77,86–93] Precise adjustment of the field frequency allows separation of various types of cells and polymer spheres in the areas of lowest and highest field intensity between electrodes.[11,94] Bennett *et al.*[95] combined negative DEP with fluid flow to achieve phase separation in particle suspensions. The suspension containing particle flows in a microfluidic channel on one side of which are situated multiple electrodes perpendicular to the channel. The particles undergoing negative DEP are barred from crossing the area of high field intensity near the electrodes, which thus serve as ''dielectrophoretic gates'' in the channel. Suehiro *et al.*[96] have demonstrated a DEP filter where yeast cells from a flowing suspension are collected and concentrated on glass beads placed in between electrodes. Local areas of high electric field intensity are created where the glass beads touch each other laterally. The yeast cells are preferentially concentrated by positive DEP in these regions. In both of these methods, switching off the field allows for the release and collection of the trapped particles and cells.

The combined action of DEP and chaining forces can be used as a tool for AC field-driven assembly of particle structures. We used alternating electric fields applied to the gap between planar electrodes for a rapid and switchable assembly of colloidal crystals from polymer and silica microspheres.[97–99] These two-dimensional crystals are specifically oriented by the field without the need for prior templating by microlithography or micromolds. Schematics of the DEP cell and images of the stages of particle assembly observed in these experiments are presented in Fig. 3. The first, rapid, stage of the crystallization is the assembly of particles in chains along the direction of the field by dipolar attraction. The particle chains are then attracted to the surface of the glass plate between the electrodes by dielectrophoresis. The chains confined to the surface assemble into hexagonal particle crystals, one axis of which is always aligned in the field direction (transverse to the electrode gap). This second slower crystallization stage is also driven by lateral attraction between the particle chains. The model for crystallization driven by a combination of induced dipole chaining and dielectrophoresis is supported both by direct microscopy observation and by reconstructing the structure from the laser diffraction pattern. The threshold field intensity for crystallization E_{th} of particles of different radii r was measured at varying frequencies and shown to form a constant group $E_{th}^2\, r^2$ = constant as expected on the basis of eqn 6.[99]

The size of these switchable 2D crystals could be larger than 25 mm^2. The laser diffraction patterns of all consecutively formed crystals are identical, which points out to the formation of a single crystal domain, unlike the multicrystalline materials assembled by convective deposition.[98,99] If the field is turned off, the arrays disassemble within seconds as the particles diffuse out of the crystal plane. Thus, the electrically tuneable crystallization can be used to make rudimentary optical switches. The transitions between ordered and

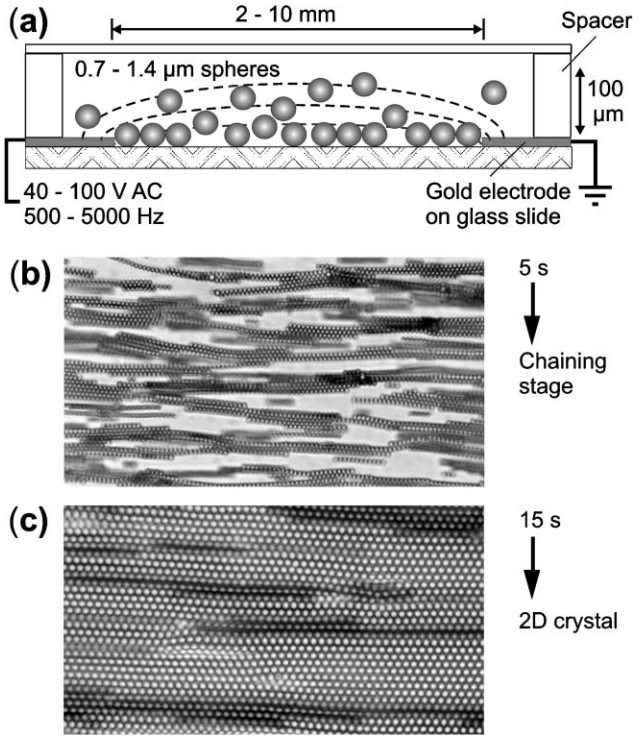

Fig. 3 Dielectrophoretic assembly of latex spheres into 2D colloidal crystals. (a) Schematics of the experimental cell designed for assembly of particles under DEP. (b) Optical micrograph taken during the initial rapid particle chaining stage. The latex spheres form chains due to dipole–dipole interactions. The chains are attracted towards the plane of electrodes by DEP, slowly merging into 2D crystals. (c) Micrograph taken after the 2D colloidal crystal is formed. The particles in the micrographs are 1.4 μm in size.

disordered states can be repeated tens of times, although the quality of the crystals in the vicinity of the electrode edges slowly degrades due to the action of the AC electrokinetic flows.

The precision of determining the lattice constant from the laser diffraction pattern is $\approx$10 nm, which allows quantifying how the electrolyte concentration can be used to tune the electrostatic repulsion between the spheres. Various combinations of DEP, EP and chaining forces are likely to find applications in more elaborate techniques for precise assembly of ordered structures.[100]

The use of AC electric fields further allows electrical measurements of the properties of captured and assembled particles, which can be used to detect target analytes present in the system. This application has been first demonstrated by Velev and Kaler, who used dielectrophoretic assembly of functionalized latex particles as a tool to make microscopic on-chip biosensors.[101] Small patches of latex particles captured and aggregated in the micrometer sized gaps between on-chip electrodes selectively bind complementary immunoglobulin molecules. The presence of captured immunoglobulin is detected by tagging with gold nanoparticles, and silver enhancement, which leads to direct electrical ''short circuiting'' of the electrodes. The result is detected by measuring the conductance of the circuit including the particle patch. More recently, silver enhancement of DNA strands functionalized with gold nanoparticles and complimentarily captured onto substrates has been used for detecting the presence of target DNA molecules.[102,103] Zheng *et al.* describe the use of a lock-in-amplifier to measure the impedance of DNA and proteins trapped under positive DEP.[104] Electric measurements and detection is a natural combination to electric field assembly that reveals the full potential of on-chip devices.

DEP manipulation of droplets from particle suspensions

Microfluidic platforms and micro- Total Analysis Systems (μTAS) are being developed for applicantions such as drug delivery, point-of-care diagnostic devices, rapid chemical syntheses and analyses, high throughput screening, biochemical and biowarfare agents detection, and water quality control.[105] These systems often require handling and manipulation of small volumes of colloidal suspensions containing solid particles, biological cells, viruses and proteins. Traditional microfluidic systems with prefabricated channels are poorly suited for flexibile and reconfigurable handling of such samples and can be severly hampered by problems such as channel clogging due to particle and cell adhesion.[106] One alternative route to ''channel-free'' μTAS is transportaion of the liquid as droplets. Various techniques for manipulation of small droplets on solid surfaces have been proposed and demonstrated.[106–111] Popular among these are the device prototypes operating on electrowetting. The applied electric field in these chips changes the contact angle of the liquid adjacent to a dielectric layer and moves the droplets by a combination of capillary effects and dielectrophoresis.[112–124] However, any system where the droplets are in contact with solid walls may encounter problems due to adsorption and fouling similar to those in conventional chips with microchannels. The surface fouling may increase the contact angle hysteresis of droplets on solid surfaces, which may increase the power dissipation and leads to heating or causes immobilization of the droplets.

These problems can be avoided by manipulating liquid droplets suspended in or floating on another immiscible liquid. A number of studies have focussed on droplet transport within microchannel devices. Droplets with diameters much smaller than the channel orifice can be formed by ''flow-focusing'' in microchannels.[125] Specially designed channels can further break up the droplets into smaller sizes.[126] Droplets flowing within channels can be diverted along different tracks by application of DEP.[127] Moreover, multiple liquid streams can be combined into single droplet whose contents are mixed rapidly without dispersion into the surrounding liquid.[128] The EHD forces acting on droplets formed using these techniques have been characterized by Zheng *et al.*[129] Such systems, however, still operate within channels and thus loose some of the flexibility required for μTAS applications.

We developed a technique where liquid microdroplets freely floating on the surface of a heavier liquid are manipulated using DEP.[130] The droplets, which may be from water or hydrocarbons, are suspended on the surface of perfluorinated hydrocarbon oil (F-oil), an inert media with high density and low dielectric permittivity. The floating droplets are manipulated by AC fields originating at arrays of electrodes below

the F-oil. The electrodes are either connected to the AC ("energized") or grounded. The dielectrophoretically trapped droplets move along programmed paths when the voltages applied to the electrodes are switched on and off consecutively. A full-scale simulation of the floating droplet geometry and electric field intensity distribution for two configurations of the energized electrode on the chip are shown in Fig. 4a. Optical microscopy images of floating 750 nL droplets containing suspended latex microspheres (top, pink) and gold nanoparticles (bottom, red) are shown in Fig. 4b. The forces operating on the droplets are purely of dielectrophoretic origin. The floating droplets are nearly submerged in the F-oil leaving only a small cap exposed to air. Since the dielectric permittivity of the droplets (ε= 80) is higher than that of the F-oil (ε = 2), they are attracted to the areas of higher field intensities.

Different equilibrium positions of the floating droplets are possible depending on the pattern of energized electrodes below them (Fig. 4). If the first electrode at the end of the array is energized, while the second and third electrodes are grounded, or alternatively, if the electrodes are energized and grounded in pairs, the floating droplet positions itself above the centre of the gap between the energized and grounded electrode(s). This places the droplet above the area of highest field intensity where the DEP force is strongest. This situation is illustrated by the left droplet in the simulation and on the real chip shown in Figs. 4a and b. However, if only a single electrode is energized in an electrode array where two neighbouring electrodes are grounded, the droplet positions itself directly above the energized electrode (see the droplet to the right in Fig. 4b). The reasons for this positioning are illustrated by the electrostatic simulation for the droplet to the right in Fig. 4a. Two areas of high field intensity are created in this electrode configuration in the gaps to the left and to the right of the energized electrode. The droplet minimizes the DEP energy by symmetrically balancing the attractive forces towards the two gaps by hovering above the electrode between them. When the electrodes in the array are turned on and off sequentially, after a droplet is captured in either configuration, the droplet moves along the path of the energized electrodes.

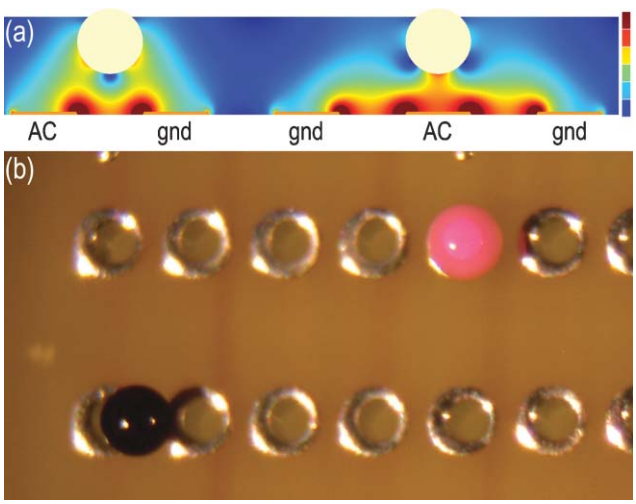

Fig. 4 On-chip manipulation of floating microdroplets using dielectrophoresis. (a) Simulation of the electric field intensity distribution in the vertical plane at two distinct droplet equilibrium positions. For electrodes energized at the end of the array, the droplet is attracted towards the middle of the gap between energized and grounded electrodes, otherwise the droplet positions itself on top of the electrode. The color scale to the right is in the order of increasing electric field intensity. (b) Optical image of 750 nl droplets (~1 mm in diameter) containing polymer microspheres (top) and gold nanoparticles (bottom) suspended above two tracks of electrodes.

These droplets are suitable for use as microreactors for chemical syntheses and can also be used for transport of the resultant precipitated solids.[130] The droplets can be further encapsulated by dodecane oil caps to prevent evaporation. Alternatively, microparticle separation and liquid circulation can be effected within evaporating droplets by Marangoni effects at the liquid surfaces. The spontaneous liquid circulation is a result of the temperature gradient caused by evaporation from the droplet surface, which in turn is coupled to an interfacial tension gradient on the droplet surface.[131] Microseparation processes were used to form anisotropic supraparticles[132] and to design immuno-agglutination microbioassays.[131] This novel microfluidic platform may find applications in chips, where single living cells or genetic material are confined into individual droplet containers, and subsequent biochemical reactions, precipitation assays, high throughput drug or toxin screening, and other biotechnological processes on the microscale are carried out. The method also illustrates the potential of dielectrophoretic techniques to affect and manipulate not only particles, but droplets and potentially a varitety of other heterogeneous systems on a chip.

Dielectrophoretic assembly of conducting particles

The assembly of conducting colloidal particles provides means for making electrical microcircuits and other functional structures such as biosensors, DNA detecting probes, *etc*. The use of dielectrophoresis offers the combination of speed, easy control and precision that might not be readily available through the more traditional colloidal assembly techniques. Quantum dots (CdSe semiconductor nanoparticles), carbon nanotubes (CNT), gold nanoparticles, DNA and protein molecules, gold nanoparticles functionalized with oligonucleotides, metal nanowires and nanorods can all be assembled using dielectrophoresis between suitably spaced electrodes. The state of the art in the preparation and use of nanoparticles in different biological, electrical and optical applications is given, *e.g.*, in recent reviews by Alivisatos[133] and Tang and Kotov.[134] The assembly of CNTs[135–143] and gold nanoparticle conjugated to DNA,[103,144] in particular, has been extensively studied due to their potential in biosensors.

We demonstrated how gold nanoparticles can be assembled into microwires using dielectrophoresis[145] and characterized the process in detail.[145,146] When AC fields of 50–100 V cm^{-1} and 100–5000 Hz frequency are applied to aqueous suspensions of 12–15 nm gold nanoparticles suspended between planar electrodes, the particles are attracted to the electrode edges where the field intensity is highest due to DEP (similar to Fig. 2b). The attracted particles aggregate and form long, porous cylindrical or half-cylindrical structures of micrometer

diameters. The microwire formation is irreversible and the assembled wires remain in the cell after removal of the applied electric field. The microwires show Ohmic conductance for both AC and DC currents and also display self-repairing behavior.[145] The rate of microwire growth was found to be controlled by diffusion-limited aggregation.[146] We observed two distinct assembly modes for gold nanoparticles in aqueous suspensions. In bulk assembly mode, the nanoparticles form cylindrical microwires through the bulk of the suspension. The microwires typically grow in a characteristic branched pattern (Fig. 5a). In surface assembly mode the microwires were assembled as half-cylinders on the surface of the glass slide.[146]

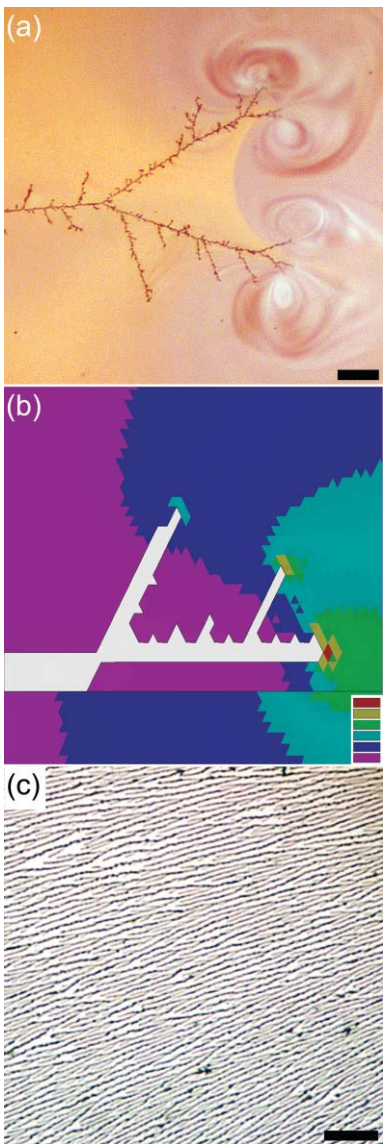

Fig. 5 Dielectrophoretic assembly of gold nanoparticles into conductive microwires. (a) Typical top-down optical micrograph of the process of bulk microwire assembly. (b) Side-view of the electrostatic simulation of bulk assembly mode—the white region represents the electrode and the growing microwire; the branching pattern predicted by the simulation is similar to the one observed experimentally in (a). (c) Parallel array of surface microwires assembled at low voltage and high frequency of the applied field. Scale bars: (a) 25 μm, (c) 5 μm.

The assembly mode of the microwires and their branching and structure can be controlled by the operating field parameters. Single bulk microwires are formed at low frequency in 1 : 1 glycerol : water suspensions, whereas parallel surface microwire arrays can be formed at low field intensity and high frequencies in aqueous suspensions.[146]

The assembly process can be simulated well by a model of an electric-field driven dielectrophoretic assembly. The electric field calculation around a growing bulk microwire in Fig. 5b points out that the field intensity is highest at the tip of the microwire. This reflects the fact that as the wire grows, it extends the electrodes into the solution (*cf.* also with Fig. 2b). The gold nanoparticles are attracted towards the growing microwire and aggregate at the tip in the areas of highest intensity. The microwires branch at the point of bifurcation of the field. Some degree of electroosmotic flow in vortices around the wire tip can also be seen in Fig. 5a, an effect commonly observed in electrodeposition. In general, however, the electrostatic model describes realistically the dynamic process and the resulting pattern of microwire assembly, including the periodic branching and self-centring on conductive objects in the media.[146]

An example of typical surface microwires grown at low voltage and high electric field frequency is shown in Fig. 5c. It was found from the simulations that the electric field intensity is always highest near the glass surface and the field-driven process may favour the formation of surface microwires. However, fluid motion at low frequencies likely disturbs this surface growth and leads to bulk wires. At higher frequencies, the AC electroosmotic fluid flow is suppressed and the nanoparticles aggregate into surface microwires. The microwires have the ability to bridge any conductive objects present in between the electrodes and to form *in situ* electrical cirucits.[145,146] The ability of electric field to assemble colloidal particles into microwires can be an important tool for nanotechnology applications such as bioelectronic interfacing of living cells to electrical circuits. The parallel surface microwires can be used in MEMS systems for one-directional heat conduction. Similar techniques have been recently developed for the assembly of gold nanoparticles and nanowires, carbon black particles and carbon nanotubes between micro electrode gaps.[147–149]

Particle and fluid manipulation by AC EHD flows

The ability of the electric fields to concentrate particles, cells or molecules of interest from dilute suspensions in μTAS devices is not only executed by dielectrophoresis and electroosmosis, but also by AC electrokinetic flows. DEP-based particle collection techniques are strongly dependent on the dielectric properties of the particles and the medium, which may be a problem in handling some types of particles. Electrokinetic flows, such as electroosmosis and AC electrohydrodynamics, are not dependent on the particle properties and thus are suitable for application in μTAS devices where the liquid, rather than the particles, is manipulated. Ramos *et al.*[1] have identified AC electrohydrodynamic flow that is generated at low frequencies (<500 kHz) on microelectrode structures. During their experiments with latex particles undergoing

positive DEP in a system with parallel finger electrodes, they observed that instead of concentrating at the electrode edges, where the field intensity is highest, the particles become collected on top of the electrodes. They attributed this flow to the interaction of the electric field with the ions in the double layer on top of the electrode. In their subsequent papers they made a detailed investigation of the EHD flow velocity as a function of field frequency and the position on the electrode and found that the particles are moving from the interelectrode gap towards the electrode.[150] The particle velocity has been highest at the electrode edge and decreased as it moved across the electrode. The velocity has also been found to depend on the frequency with a maximum occurring at a characteristic frequency and tending to zero at low and high frequencies. It has been established that the EHD flow velocity is dependent on the square of the applied voltages in systems with low conductivities.[151] A detailed theoretical model based on the assumption of a thin double layer formation on the electrodes has been developed, and scaling laws for the various forces acting on particles suspended in a microelectrode system with applied AC field have been established. It has been concluded that EHD is the dominant force at low frequencies and for small system sizes.[152] Electrothermal forces, which occur due to the temperature dependent changes in the permittivity and conductivity of the suspension, dominate at high frequency and high voltages. In most μTAS EHD systems, thus, it is advisable to work at low to moderate frequencies and at low voltages to prevent electrothermal effects. A novel technique to independently measure the particle and liquid velocity in electrokinetic systems using two colour micro-particle image velocimetry (μPIV) has been recently developed by Wang *et al.*[153] It allows decoupling the DEP contribution to particle velocity from the EHD and electro-thermal contributions.

Various particle-trapping techniques that use AC EHD have been developed. Chang *et al.*[154–156] designed impedance spectroscopy detectors that take advantage of AC EHD to rapidly concentrate bioparticles, leading to enhanced sensitivity due to reduction of the transport time to the detector. Chip designs that combine DEP with EHD flow for particle concentration have been extended by Hoettges *et al.*[157] and Wong *et al.*[158] Frequency-dependent EHD flows and EO roll cells, combined with DEP forces have been used by Zhou *et al.* to collect yeast cells and latex particles into controlled patterns between interdigitated electrodes.[159]

Another important application of EHD flow in μTAS is pumping fluids.[160,161] The use of EHD instead of electro-osmosis requires lower voltages, and also prevents electrolysis and bubble formation in the suspension. However, as AC fields create roll flows on top of electrodes, it is essential to design electrode configurations that generate a net fluid flow in the device. Several such designs have been proposed and implemented. Ajdari[162] detailed the formation of fluid rolls on a charge-modulated surface in presence of an applied external field. He proposed the use of an undulated surface close to the charge-modulated surface to create biased rolls, leading to a net flow in the channel formed by the two surfaces. Asymmetric electrode arrays can be used to break the symmetry of the rolls created in EHD.[163,164] A practical demonstration of using asymmetric electrode for pumping water in microfluidic channel was presented by Brown *et al.*[165] Interdigitated electrodes with a large electrode followed by small gap and a small electrode followed by a large gap lead to a net flow of fluid from the large electrode towards the small electrode across the large gap. A further improvement of the performance of the system was achieved by placing two interdigitated electrode arrays, one on the top and one on the bottom of the system.[166] Fluid velocities in excess of 450 μm s^{-1} were obtained in channels of 280 μm gaps. Debesset *et al.*[167] developed an AC electroosmotic micropump that works by placing interdigitated electrodes in a circular channel. This makes it useful for circular chromatography applications, which require a closed loop system. Furthermore, micro-vortexes for mixing applications can be generated electroosmotically in channels with patterned walls or at microchannel junctions.[168–171]

We identified an electrohydrodynamics effect arising from the application of AC fields between two patterned electrodes facing each other in a thin chamber.[172] The schematics of our experimental system are shown in Fig. 6a. An electric field was applied to latex particles suspended between a patterned silicon electrode and an indium–tin oxide (ITO) coated glass slide separated vertically by a 0.75 mm spacer. To fabricate the bottom electrode, a conductive silicon wafer was covered with a 1 μm thick layer of insulating photoresist. The photoresist was patterned using standard photolithography tools to expose 1 mm^2 square corrals of the underlying silicon wafer. When an AC field is applied to the top and bottom electrodes, a fluid flow at the photoresist-silicon wafer edge emerges, resulting in the collection of the suspended particles in a neat "pile" in the centre of the conductive corrals as shown in Fig. 6b.

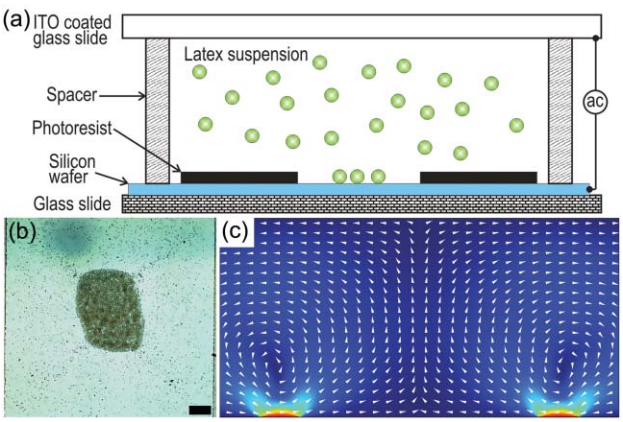

Fig. 6 Particle collection and concentration in a thin chamber with patterned electrodes using AC electrohydrodynamics. (a) Schematic of the experimental chip. (b) Typical optical micrograph of yeast cells collected at the center of the conductive "corral". Scale bar: 100 μm. (c) Simulation of the fluid velocity distribution in the experimental chamber. Arrows indicate the direction of the fluid flow and the colors indicate the magnitude with red being the highest fluid velocity. The simulation shows how the local EHD flow generated at the photoresist-conductive corral edge leads to bulk fluid flow throughout the chamber. All particles are collected at the stagnation region in the center of the corral.

The mechanism behind this particle collection process was found to be field-induced EHD flow similar to that discussed above and in the introductory section. Electrical double layers are formed on the conducting silicon wafer surface and the ITO covered glass slide, with charge opposite to that of the applied voltage of the electrode. An electrical double layer is also formed on the photoresist surface. The voltage applied to the silicon wafer beneath the dielectric layer creates an oppositely charged double layer on the photoresist–electrolyte interface by means of the photoresist layer acting as a capacitor. The tangential electric field is zero on the conductive silicon wafer patches and the ITO electrode. However, a tangential electric field that induces EHD is present on the photoresist surface near the corrals and reaches its maximum at the polymer edge. This gradient generates the EHD flow. For different half-cycles of the electric field, the sign of the induced charge and the sign of the electric field change concurrently, and thus the EHD flow is always in the same direction leading to particle transport towards the centre of the corrals. This strong EHD flow (in some instances > 50 μm s^{-1}) leads to formation of electroosmotic flow roll cells throughout the chamber as simulated in Fig. 6c. The colours indicate the magnitude of the velocity with red being the highest, while the white arrows indicate the direction of the flow. Particles throughout the chamber are dragged by this flow and deposited at the stagnation regions in the centre of the conductive corrals.

The EHD flow near the corral edges scales with the square of the applied voltage. This is to be expected since both the induced potential and the induced field depend on the voltage and thus from eqn 7, the EHD flow should scale with applied voltage squared. As the frequency of the electric field is increased, the ions in the solution do not have enough time to form a double layer when the field changes signs. This leads to strong suppression of the EHD flow at frequencies above 5000 Hz. At very low frequencies, the entire potential drop takes place within the double layer and hence there is no electric field in the bulk solution. Thus, the EHD flow regime was found to be operating only between 10–5000 Hz. On addition of higher concentrations of electrolyte (equivalent to 2 mM NaCl) the EHD flow disappears as the potential is again dropped in the double layer, similar to the low frequency case. All of these trends are in good correspondence to the literature on EHD.[2,153–159,173] For lower concentrations of electrolyte there is no change in the EHD effect. The electrolyte, however, increases the adhesion of collected latex particle to the silicon surface due to a decrease in the electrostatic repulsion forces.

This technique is promising for various devices that collect and analyze particles on a chip. We demonstrated that such devices could be used, for example, to collect yeast cells and microbes from dilute water suspensions. In more general plan, devices for particle collection could use a combination of DEP, AC electrokinetics and DC electroosmosis in new synergistic ways. Such chips are presently under development by many groups.

Conclusions

The investigation and development of techniques for particle manipulation and assembly based on electric fields has been briefly overviewed here with the specific focus on particle handling and assembly in aqueous environments. The effects involved, and the possible on-chip electrode configurations are numerous and still largely unexplored. An interesting area of research could be the dielectrophoretic response of particles of non-spherical shape, non-isotropic charge or surface composition, permanently embedded dipole moment or non-linear conductance. Experimental studies in this area are generally lacking, not in the least because few methods for the fabrication of such complex particles have been available. Recent advances in the area of making complex anisotropic particles, ''supraparticles'' and ''colloidal molecules'' are likely to make possible research on the dielectrophoretic and electrokinetic properties of such particles and reveal new effects and applications.

A large pool of potential applications is likely to emerge with the rapid progress in the area of microfluidic and bioassay devices. In addition to the established techniques for on-chip characterization and separation of cells, dielectrophoretic and electrokinetic methods are likely to find much larger use in the on-chip handling and separation of proteins and DNA. The electric field driven assembly of cells and nanoparticles can be used to create new types of biosensors, microbioassays and bioelectronic circuits. The AC electrokinetic effects are still incompletely understood on the microscopic (particle) scale and for the cases of more complex electrode and experimental cell designs. Many new lab-on-a-chip applications are likely to use AC electrokinetic techniques for liquid handling, as well as for particle collection and manipulation. Interesting new developments will probably come from the discovery of new AC dielectrophoretic and electrokinetic effects and from better theoretical interpretation of complex liquid mediated particle–particle interactions. The convergence of electrical micro-circuits and soft colloidal materials is forthcoming and its technology potential is still largely unexplored.

Acknowledgements

This work was supported by CAREER, NER and NIRT grants from the National Science Foundation, USA. We are thankful to our collaborators from North Carolina State University, University of Delaware and RTI International, including Simon Lumsdon, Eric Kaler, Kevin Hermanson, Brian Prevo, Jeffrey Millman and Sonia Grego.

References

1 A. Ramos, H. Morgan, N. G. Green and A. Castellanos, *J. Phys. D: Appl. Phys.*, 1998, **31**, 2338–2353.
2 R. J. Hunter, *Foundations of colloid science*, 2nd edn., Oxford University Press, Oxford, 2001.
3 J. Lyklema, *J. Colloid Interface Sci.*, 1977, **58**, 242–250.
4 D. F. Evans and H. Wennerstrom, *The colloidal domain: where physics, chemistry and biology meet*, 2nd edn., John Wiley & Sons Inc, New York, 1999.
5 H. Ohshima, *J. Colloid Interface Sci.*, 1996, **180**, 299–301.
6 R. W. O'Brien and L. R. White, *J. Chem. Soc., Faraday Trans. 2*, 1978, **74**, 1607–1626.
7 D. P. J. Barz and P. Ehrhard, *Lab Chip*, 2005, **5**, 949–958.
8 P. J. Sides, *Langmuir*, 2001, **17**, 5791–5800.
9 H. A. Pohl, *J. Appl. Phys.*, 1951, **22**, 869–871.
10 T. B. Jones, *Electromechanics of particles*, Cambridge University Press, Cambridge, 1995.

11 R. Pethig, Y. Huang, X. B. Wang and J. P. H. Burt, *J. Phys. D: Appl. Phys.*, 1992, **25**, 881–888.
12 T. Muller, A. Gerardino, T. Schnelle, S. G. Shirley, F. Bordoni, G. DeGasperis, R. Leoni and G. Fuhr, *J. Phys. D: Appl. Phys.*, 1996, **29**, 340–349.
13 G. Fuhr, T. Muller, T. Schnelle, R. Hagedorn, A. Voigt, S. Fiedler, W. M. Arnold, U. Zimmermann, B. Wagner and A. Heuberger, *Naturwissenschaften*, 1994, **81**, 528–535.
14 C. S. Mangelsdorf and L. R. White, *J. Chem. Soc., Faraday Trans.*, 1990, **86**, 2859–2870.
15 C. S. Mangelsdorf and L. R. White, *J. Chem. Soc., Faraday Trans.*, 1992, **88**, 3567–3581.
16 H. Zhou, M. A. Preston, R. D. Tilton and L. R. White, *J. Colloid Interface Sci.*, 2005, **285**, 845–856.
17 H. Zhou, M. A. Preston, R. D. Tilton and L. R. White, *J. Colloid Interface Sci.*, 2005, **292**, 277–289.
18 R. Pethig, Institute of Physics Conference Series, 1991.
19 J. P. Huang, K. W. Yu, G. Q. Gu and M. Karttunen, *Phys. Rev. E: Stat. Phys., Plasmas, Fluids, Relat. Interdiscip. Top.*, 2003, **67**, 021403.
20 B. Malyan and W. Balachandran, *J. Electrost.*, 2001, **51**, 15–19.
21 M. P. Hughes, *Nanotechnology*, 2000, **11**, 124–132.
22 V. Giner, M. Sancho, R. S. Lee, G. Martinez and R. Pethig, *J. Phys. D: Appl. Phys.*, 1999, **32**, 1182–1186.
23 R. Kretschmer and W. Fritzsche, *Langmuir*, 2004, **20**, 11797–11801.
24 M. Z. Bazant and T. M. Squires, *Phys. Rev. Lett.*, 2004, **92**, 066101.
25 T. M. Squires and M. Z. Bazant, *J. Fluid Mech.*, 2004, **509**, 217–252.
26 J. Lyklema, *Fundmentals of interface and colloid science 2: solid–liquid interfaces*, Academic Press Inc., San Diego, 1995.
27 H. Morgan and N. G. Green, *AC electrokinetics: colloids and nanoparticles*, Research Studies Press, Baldock, 2001.
28 M. Giersig and P. Mulvaney, *Langmuir*, 1993, **9**, 3408–3413.
29 M. Holgado, F. Garcia-Santamaria, A. Blanco, M. Ibisate, A. Cintas, H. Miguez, C. J. Serna, C. Molpeceres, J. Requena, A. Mifsud, F. Meseguer and C. Lopez, *Langmuir*, 1999, **15**, 4701–4704.
30 A. L. Rogach, N. A. Kotov, D. S. Koktysh, J. W. Ostrander and G. A. Ragoisha, *Chem. Mater.*, 2000, **12**, 2721–2726.
31 R. C. Bailey, K. J. Stevenson and J. T. Hupp, *Adv. Mater.*, 2000, **12**, 1930–1934.
32 J. Sun, M. Gao and J. Feldman, *J. Nanosci. Nanotechnol.*, 2001, **1**, 133–136.
33 Z. Z. Gu, S. Hayami, S. Kubo, Q. B. Meng, Y. Einaga, D. A. Tryk, A. Fujishima and O. Sato, *J. Am. Chem. Soc.*, 2001, **123**, 175–176.
34 M. Gao, J. Sun, E. Dulkeith, N. Gaponik, U. Lemmer and J. Feldman, *Langmuir*, 2002, **18**, 4098–4102.
35 Y. C. Wang, I. C. Leu and M. H. Hon, *J. Mater. Chem.*, 2002, **12**, 2439–2444.
36 R. J. Kershner, J. W. Bullard and M. J. Cima, *J. Colloid Interface Sci.*, 2004, **278**, 146–154.
37 R. K. Golding, P. C. Lewis and E. Kumacheva, *Langmuir*, 2004, **20**, 1414–1419.
38 W. M. Choi and O. Park, *Nanotechnology*, 2006, **17**, 325–329.
39 N. Wang, H. Lin, J. B. Li, X. Z. Yang and B. Chi, *Thin Solid Films*, 2006, **496**, 649–652.
40 B. Comiskey, J. D. Albert, H. Yoshizawa and J. Jacobson, *Nature*, 1998, **394**, 253–255.
41 J. A. Rogers, Z. Bao, K. Baldwin, A. Dodabalapur, B. Crone, V. R. Raju, V. Kuck, H. Katz, K. Amundson, J. Ewing and P. Drzaic, *Proc. Natl. Acad. Sci. U. S. A.*, 2001, **98**, 4835–4840.
42 M. Trau, D. A. Saville and I. A. Aksay, *Science*, 1996, **272**, 706–709.
43 M. Trau, D. A. Saville and I. A. Aksay, *Langmuir*, 1997, **13**, 6375–6381.
44 M. Bohmer, *Langmuir*, 1996, **12**, 5747–5750.
45 Y. Solomentsev, M. Bohmer and J. L. Anderson, *Langmuir*, 1997, **13**, 6058–6068.
46 Y. Solomentsev, S. A. Guelcher, M. Bevan and J. L. Anderson, *Langmuir*, 2000, **16**, 9208–9216.
47 J. Kim, S. A. Guelcher, S. Garoff and J. L. Anderson, *Adv. Colloid Interface Sci.*, 2002, **96**, 131–142.
48 J. Kim, J. L. Anderson, S. Garoff and P. J. Sides, *Langmuir*, 2002, **18**, 5387–5391.
49 P. Richetti, J. Prost and P. Barois, *J. Phys. Lett.*, 1984, **45**, 1137–1143.
50 S. R. Yeh, M. Seul and B. I. Shraiman, *Nature*, 1997, **386**, 57–59.
51 C. Faure, N. Decoster and F. Argoul, *Eur. Phys. J. B*, 1998, **5**, 87–97.
52 F. Nadal, F. Argoul, P. Hanusse, B. Pouligny and A. Ajdari, *Phys. Rev. E: Stat. Phys., Plasmas, Fluids, Relat. Interdiscip. Top.*, 2002, **65**, 061409.
53 F. Nadal, F. Argoul, P. Kestener, B. Pouligny, C. Ybert and A. Ajdari, *Eur. Phys. J. E*, 2002, **9**, 387–399.
54 W. D. Ristenpart, I. A. Aksay and D. A. Saville, *Phys. Rev. Lett.*, 2003, **90**, 128303.
55 W. D. Ristenpart, I. A. Aksay and D. A. Saville, *Phys. Rev. E: Stat. Phys., Plasmas, Fluids, Relat. Interdiscip. Top.*, 2004, **69**, 021405.
56 T. Gong and D. W. M. Marr, *Langmuir*, 2001, **17**, 2301–2304.
57 T. Gong, D. T. Wu and D. W. M. Marr, *Langmuir*, 2002, **18**, 10064–10067.
58 T. Y. Gong, D. T. Wu and D. W. M. Marr, *Langmuir*, 2003, **19**, 5967–5970.
59 R. C. Hayward, D. A. Saville and I. A. Aksay, *Nature*, 2000, **404**, 56–59.
60 J. L. Anderson, J. Kim, S. Garoff and P. J. Sides, *International conference on electrophoretic deposition, fundamentals and applications*, Banff, Canada, 2002.
61 J. A. Fagan, P. J. Sides and P. C. Prieve, *Langmuir*, 2002, **18**, 7810–7820.
62 P. J. Sides, *Langmuir*, 2003, **19**, 2745–2751.
63 J. A. Fagan, P. J. Sides and D. C. Prieve, *Langmuir*, 2003, **19**, 6627–6632.
64 J. A. Fagan, P. J. Sides and D. C. Prieve, *Langmuir*, 2004, **20**, 4823–4834.
65 J. A. Fagan, P. J. Sides and D. C. Prieve, *Langmuir*, 2005, **21**, 1784–1794.
66 M. Washizu and O. Kurosawa, *IEEE Trans. Ind. Appl.*, 1990, **26**, 1165–1172.
67 M. Washizu, M. Suzuki, O. Kurosawa, T. Nishizaka and T. Shinohara, *IEEE T. Ind. Appl.*, 1994, **30**, 835–843.
68 M. Washizu, O. Kurosawa, I. Arai, S. Suzuki and N. Shimamoto, *IEEE T. Ind. Appl.*, 1995, **31**, 447–456.
69 S. Suzuki, T. Yamanashi, S. Tazawa, O. Kurosawa and M. Washizu, *IEEE T. Ind. Appl.*, 1998, **34**, 75–83.
70 T. Kawabata and M. Washizu, *IEEE T. Ind. Appl.*, 2001, **37**, 1625–1633.
71 C. L. Asbury, A. H. Diercks and G. van den Engh, *Electrophoresis*, 2002, **23**, 2658–2666.
72 C. F. Chou, J. O. Tegenfeldt, O. Bakajin, S. S. Chan, E. C. Cox, N. Darnton, T. Duke and R. H. Austin, *Biophys. J.*, 2002, **83**, 2170–2179.
73 G. Fuhr, W. M. Arnold, R. Hagedorn, T. Muller, W. Benecke, B. Wagner and U. Zimmermann, *Biochim. Biophys. Acta*, 1992, **1108**, 215–223.
74 S. Fiedler, S. G. Shirley, T. Schnelle and G. Fuhr, *Anal. Chem.*, 1998, **70**, 1909–1915.
75 V. Brisson and R. D. Tilton, *Biotechnol. Bioeng.*, 2002, **77**, 290–295.
76 T. Heida, W. L. C. Rutten and E. Marani, *J. Phys. D: Appl. Phys.*, 2002, **35**, 1592–1602.
77 Y. Huang, S. Joo, M. Duhon, M. Heller, B. Wallace and X. Xu, *Anal. Chem.*, 2002, **74**, 3362–3371.
78 P. Gascoyne, C. Mahidol, M. Ruchirawat, J. Satayavivad, P. Watcharasit and F. F. Becker, *Lab Chip*, 2002, **2**, 70–75.
79 A. R. Minerick, A. E. Ostafin and H. C. Chang, *Electrophoresis*, 2002, **23**, 2165–2173.
80 A. R. Minerick, R. H. Zhou, P. Takhistov and H. C. Chang, *Electrophoresis*, 2003, **24**, 3703–3717.
81 M. Frenea, S. P. Faure, B. Le Pioufle, P. Coquet and H. Fujita, *Mater. Sci. Eng., C*, 2003, **23**, 597–603.
82 S. Prasad, M. Yang, X. Zhang, C. S. Ozkan and M. Ozkan, *Biomed. Microdevices*, 2003, **5**, 125–137.
83 N. Manaresi, A. Romani, G. Medoro, L. Altomare, A. Leonardi, M. Tartagni and R. Guerrieri, *IEEE J. Solid-State Circuits*, 2003, **38**, 2297–2305.

84 C. E. Verduzco-Luque, B. Alp, G. M. Stephens and G. H. Markx, *Biotechnol. Bioeng.*, 2003, **83**, 39–44.
85 D. S. Gray, J. L. Tan, J. Voldman and C. S. Chen, *Biosens. Bioelectron.*, 2004, **19**, 1765–1774.
86 H. A. Pohl and I. Hawk, *Science*, 1966, **152**, 647–649.
87 Y. Huang, R. Holzel, R. Pethig and X. B. Wang, *Phys. Med. Biol.*, 1992, **37**, 1499–1517.
88 Y. Huang, X. B. Wang, F. F. Becker and P. Gascoyne, *Biophys. J.*, 1997, **73**, 1118–1129.
89 A. Docoslis, N. Kalogerakis, L. A. Behie and K. Kaler, *Biotechnol. Bioeng.*, 1997, **54**, 239–250.
90 P. R. C. Gascoyne and J. Vykoukal, *Electrophoresis*, 2002, **23**, 1973–1983.
91 J. Suehiro, R. Hamada, D. Noutomi, M. Shutou and M. Hara, *J. Electrost.*, 2003, **57**, 157–168.
92 J. Astorga-Wells, S. Vollmer, S. Tryggvason, T. Bergman and H. Jornvall, *Anal. Chem.*, 2005, **77**, 7131–7136.
93 M. R. King, O. A. Lomakin, R. Ahmed and T. B. Jones, *J. Appl. Phys.*, 2005, **97**, 054902.
94 J. Auerswald and H. F. Knapp, *Microelectron. Eng.*, 2003, **67–8**, 879–886.
95 D. J. Bennett, B. Khusid, C. D. James, P. C. Galambos, M. Okandan, D. Jacqmin and A. Acrivos, *Appl. Phys. Lett.*, 2003, **83**, 4866–4868.
96 J. Suehiro, G. B. Zhou, M. Imamura and M. Hara, *IEEE. T. Ind. Appl.*, 2003, **39**, 1514–1521.
97 O. D. Velev and S. O. Lumsdon, in *Handbook of surfaces and interfaces of materials*, ed. H. S. Nalwa, Academic Press, San Diego, 2002, vol. 3, pp. 125–163.
98 S. O. Lumsdon, E. W. Kaler, J. P. Williams and O. D. Velev, *Appl. Phys. Lett.*, 2003, **82**, 949–951.
99 S. O. Lumsdon, E. W. Kaler and O. D. Velev, *Langmuir*, 2004, **20**, 2108–2116.
100 O. D. Velev, in *Colloids and colloid assemblies*, ed. F. Caruso, Wiley VCH, Weinheim, 2004.
101 O. D. Velev and E. W. Kaler, *Langmuir*, 1999, **15**, 3693–3698.
102 R. Moller, A. Csaki, J. M. Kohler and W. Fritzsche, *Langmuir*, 2001, **17**, 5426–5430.
103 S. J. Park, T. A. Taton and C. A. Mirkin, *Science*, 2002, **295**, 1503–1506.
104 L. F. Zheng, J. P. Brody and P. J. Burke, *Biosens. Bioelectron.*, 2004, **20**, 606–619.
105 H. A. Stone and S. Kim, *AIChE J.*, 2001, **47**, 1250–1254.
106 M. K. Chaudhury and G. M. Whitesides, *Science*, 1992, **256**, 1539–1541.
107 K. Hosokawa, T. Fujii and I. Endo, *Anal. Chem.*, 1999, **71**, 4781–4785.
108 J. Y. Shin and N. L. Abbott, *Langmuir*, 1999, **15**, 4404–4410.
109 S. W. Lee and P. E. Laibinis, *J. Am. Chem. Soc.*, 2000, **122**, 5395–5396.
110 K. Ichimura, S. K. Oh and M. Nakagawa, *Science*, 2000, **288**, 1624–1626.
111 S. Daniel and M. K. Chaudhury, *Langmuir*, 2002, **18**, 3404–3407.
112 J. L. Jackel, S. Hackwood and G. Beni, *Appl. Phys. Lett.*, 1982, **40**, 4–6.
113 M. Washizu, *IEEE T. Ind. Appl.*, 1998, **34**, 732–737.
114 J. H. Lee and C. J. Kim, *J. Microelectromech. S.*, 2000, **9**, 171–180.
115 B. S. Gallardo, V. K. Gupta, F. D. Eagerton, L. I. Jong, V. S. Craig, R. R. Shah and N. L. Abbott, *Science*, 1999, **283**, 57–60.
116 T. B. Jones, M. Gunji, M. Washizu and M. J. Feldman, *J. Appl. Phys.*, 2001, **89**, 1441–1448.
117 T. B. Jones, *J. Electrost.*, 2001, **51**, 290–299.
118 M. G. Pollack, A. D. Shenderov and R. B. Fair, *Lab Chip*, 2002, **2**, 96–101.
119 T. B. Jones, *Langmuir*, 2002, **18**, 4437–4443.
120 L. Latorre, J. W. Kim, J. H. Lee, P. P. de Guzman, H. J. Lee, P. Nouet and C. J. Kim, *J. Microelectromech. S.*, 2002, **11**, 302–308.
121 S. K. Cho, H. Moon and C. J. Kim, *J. Microelectromech. Syst.*, 2003, **12**, 70–80.
122 J. A. Schwartz, J. V. Vykoukal and P. R. C. Gascoyne, *Lab Chip*, 2004, **4**, 11–17.
123 L. Y. Yeo and H. C. Chang, *Mod. Phys. Lett. B*, 2005, **19**, 549–569.
124 L. Y. Yeo and H. C. Chang, *Phys. Rev. E: Stat. Phys., Plasmas, Fluids, Relat. Interdiscip. Top.*, 2006, **73**, 011605.
125 S. L. Anna, N. Bontoux and H. A. Stone, *Appl. Phys. Lett.*, 2003, **82**, 364–366.
126 D. R. Link, S. L. Anna, D. A. Weitz and H. A. Stone, *Phys. Rev. Lett.*, 2004, **92**, 054503.
127 K. Ahn, C. Kerbage, T. P. Hunt, R. M. Westervelt, D. R. Link and D. A. Weitz, *Appl. Phys. Lett.*, 2006, **88**, 024104.
128 H. Song, J. D. Tice and R. F. Ismagilov, *Angew. Chem., Int. Ed.*, 2003, **42**, 767–772.
129 J. Zeng and T. Korsmeyer, *Lab Chip*, 2004, **4**, 265–277.
130 O. D. Velev, B. G. Prevo and K. H. Bhatt, *Nature*, 2003, **426**, 515–516.
131 S. T. Chang and O. D. Velev, *Langmuir*, 2006, **22**, 1459–1468.
132 J. R. Millman, K. H. Bhatt, B. G. Prevo and O. D. Velev, *Nat. Mater.*, 2005, **4**, 98–102.
133 A. P. Alivisatos, *Nat. Biotechnol.*, 2004, **22**, 47–52.
134 Z. Y. Tang and N. A. Kotov, *Adv. Mater.*, 2005, **17**, 951–962.
135 K. Yamamoto, S. Akita and Y. Nakayama, *J. Phys. D: Appl. Phys.*, 1998, **31**, L34–L36.
136 G. L. Che, B. B. Lakshmi, E. R. Fisher and C. R. Martin, *Nature*, 1998, **393**, 346–349.
137 C. Liu, Y. Y. Fan, M. Liu, H. T. Cong, H. M. Cheng and M. S. Dresselhaus, *Science*, 1999, **286**, 1127–1129.
138 J. Kong, M. G. Chapline and H. G. Dai, *Adv. Mater.*, 2001, **13**, 1384–1386.
139 X. Q. Chen, T. Saito, H. Yamada and K. Matsushige, *Appl. Phys. Lett.*, 2001, **78**, 3714–3716.
140 H. J. Dai, *Surf. Sci.*, 2002, **500**, 218–241.
141 R. H. Baughman, A. A. Zakhidov and W. A. de Heer, *Science*, 2002, **297**, 787–792.
142 Q. Zhao, Z. H. Gan and Q. K. Zhuang, *Electroanalysis*, 2002, **14**, 1609–1613.
143 R. Krupke, F. Hennrich, H. B. Weber, M. M. Kappes and H. von Lohneysen, *Nano Lett.*, 2003, **3**, 1019–1023.
144 E. Braun, Y. Eichen, U. Sivan and G. Ben-Yoseph, *Nature*, 1998, **391**, 775–778.
145 K. D. Hermanson, S. O. Lumsdon, J. P. Williams, E. W. Kaler and O. D. Velev, *Science*, 2001, **294**, 1082–1086.
146 K. H. Bhatt and O. D. Velev, *Langmuir*, 2004, **20**, 467–476.
147 S. O. Lumsdon and D. M. Scott, *Langmuir*, 2005, **21**, 4874–4880.
148 P. A. Smith, C. D. Nordquist, T. N. Jackson, T. S. Mayer, B. R. Martin, J. Mbindyo and T. E. Mallouk, *Appl. Phys. Lett.*, 2000, **77**, 1399–1401.
149 S. I. Khondaker and Z. Yao, *Appl. Phys. Lett.*, 2002, **81**, 4613–4615.
150 A. Ramos, H. Morgan, N. G. Green and A. Castellanos, *J. Colloid Interface Sci.*, 1999, **217**, 420–422.
151 A. Gonzalez, A. Ramos, N. G. Green, A. Castellanos and H. Morgan, *Phys. Rev. E: Stat. Phys., Plasmas, Fluids, Relat. Interdiscip. Top.*, 2000, **61**, 4019–4028.
152 A. Castellanos, A. Ramos, A. Gonzalez, N. G. Green and H. Morgan, *J. Phys. D: Appl. Phys.*, 2003, **36**, 2584–2597.
153 D. Z. Wang, M. Sigurdson and C. D. Meinhart, *Exp. Fluids*, 2005, **38**, 1–10.
154 J. Wu, Y. X. Ben, D. Battigelli and H. C. Chang, *Ind. Eng. Chem. Res.*, 2005, **44**, 2815–2822.
155 J. Wu, Y. X. Ben and H. C. Chang, *Microfluid. Nanofluid.*, 2005, **1**, 161–167.
156 Z. Gagnon and H. C. Chang, *Electrophoresis*, 2005, **26**, 3725–3737.
157 K. F. Hoettges, M. B. McDonnell and M. P. Hughes, *J. Phys. D: Appl. Phys.*, 2003, **36**, L101–L104.
158 P. K. Wong, C. Y. Chen, T. H. Wang and C. M. Ho, *Anal. Chem.*, 2004, **76**, 6908–6914.
159 H. Zhou, L. R. White and R. D. Tilton, *J. Colloid Interface Sci.*, 2005, **285**, 179–191.
160 H. A. Stone, A. D. Stroock and A. Ajdari, *Annu. Rev. Fluid Mech.*, 2004, **36**, 381–411.
161 L. Bousse, C. Cohen, T. Nikiforov, A. Chow, A. R. Kopf-Sill, R. Dubrow and J. W. Parce, *Annu. Rev. Bioph. Biom.*, 2000, **29**, 155–181.
162 A. Ajdari, *Phys. Rev. Lett.*, 1995, **75**, 755–758.

163 A. Ajdari, *Phys. Rev. E: Stat. Phys., Plasmas, Fluids, Relat. Interdiscip. Top.*, 2000, **61**, R45–R48.
164 A. Ajdari, *Appl. Phys. A: Mater. Sci. Process.*, 2002, **75**, 271–274.
165 A. B. D. Brown, C. G. Smith and A. R. Rennie, *Phys. Rev. E: Stat. Phys., Plasmas, Fluids, Relat. Interdiscip. Top.*, 2001, **6302**, 016305.
166 M. Mpholo, C. G. Smith and A. B. D. Brown, *Sens. Actuators, B*, 2003, **92**, 262–268.
167 S. Debesset, C. J. Hayden, C. Dalton, J. C. T. Eijkel and A. Manz, *Lab Chip*, 2004, **4**, 396–400.
168 S. K. Thamida and H. C. Chang, *Phys. Fluids*, 2002, **14**, 4315–4328.
169 P. Takhistov, K. Duginova and H. C. Chang, *J. Colloid Interface Sci.*, 2003, **263**, 133–143.
170 S. C. Wang, Y. W. Lai, Y. X. Ben and H. C. Chang, *Ind. Eng. Chem. Res.*, 2004, **43**, 2902–2911.
171 P. Wang, Z. L. Chen and H. C. Chang, *Sens. Actuators, B*, 2006, **113**, 500–509.
172 K. H. Bhatt, S. Grego and O. D. Velev, *Langmuir*, 2005, **21**, 6603–6612.
173 N. G. Green, A. Ramos, A. Gonzalez, H. Morgan and A. Castellanos, *Phys. Rev. E: Stat. Phys., Plasmas, Fluids, Relat. Interdiscip. Top.*, 2000, **61**, 4011–4018.

